JAERI-Tech
2002-039

VXIbus-BASED SIGNAL GENERATOR FOR RESONANT POWER SUPPLY SYSTEM OF THE 3 GeV RCS

March 2002

Fengqing ZHANG, Yasuhiro WATANABE, Shoichiro KOSEKI,
Norio TANI, Toshikazu ADACHI* and Hirohiko SOMEYA*

日本原子力研究所
Japan Atomic Energy Research Institute

本レポートは，日本原子力研究所が不定期に公刊している研究報告書です。
入手の問合わせは，日本原子力研究所研究情報部研究情報課（〒319－1195 茨城県那珂郡東海村）あて，お申し越しください。なお，このほかに財団法人原子力弘済会資料センター（〒319－1195 茨城県那珂郡東海村日本原子力研究所内）で複写による実費頒布をおこなっております。

This report is issued irregularly.
Inquiries about availability of the reports should be addressed to Research Information Division, Department of Intellectual Resources, Japan Atomic Energy Research Institute, Tokai-mura, Naka-gun, Ibaraki-ken 〒319－1195, Japan.

編集兼発行　日本原子力研究所

JAERI-Tech 2002-039

VXIbus-based Signal Generator for Resonant Power Supply System of the 3 GeV RCS

Fengqing ZHANG, Yasuhiro WATANABE, Shoichiro KOSEKI※, Norio TANI,
Toshikazu ADACHI* and Hirohiko SOMEYA*

Center for Neutron Science
Tokai Research Establishment
Japan Atomic Energy Research Institute
Tokai-mura, Naka-gun, Ibaraki-ken

(Received February 1, 2002)

The 3 GeV Proton RCS of the JAERI-KEK Joint Project is a 25 Hz separate-function rapid cycling synchrotron under design. Bending magnets (BM) and quadrupole magnets (QM) are excited separately. The 3 GeV RCS requests above 10 families of magnets excited independently, far beyond 3 families in practical RCS's. Difficulty of field tracking between BM and QM is significantly increased.

Magnet strings are grouped into resonant networks and excited resonantly with power supplies driven by a waveform pattern, typically a DC-biased sinusoidal signal. To achieve a close tracking between many families, the driving signal of each power supply should be adjusted in phase and amplitude flexibly and dynamically.

This report proposes a signal generator based on VXIbus. The VXIbus, an extension of VMEbus (VME eXtensions for Instrument), provides an open architecture with shared process bus and timing. The VXIbus-based signal generator facilitates the timing synchronization and is easy to extend to many channels needed by the 3 GeV RCS. Experimental results of the signal generator are reported.

Keywords: Joint Project, 3GeV Synchrotron, Resonant Power Supplies, Signal Generator, Tracking

---

※ On leave from Hitachi, Ltd.

* High Energy Accelerator Research Organization

VXIbus を用いた 3GeV RCS 共振電源信号発生器

日本原子力研究所東海研究所中性子科学研究センター
張　鳳清・渡辺　泰広・古関　庄一郎※・谷　教夫・安達　利一*・染谷　宏彦*

(2002 年 2 月 1 日 受理)

JAERI-KEK 大強度陽子加速器統合計画の 3GeV シンクロトロンの設計は，スケジュールどおりに進行中である。この 3GeV 陽子加速器は，機能分離型のラピッド・サイクリング・シンクロトロン(RCS)であり，偏向電磁石(BM)および四極電磁石(QM)は，DC バイアスされた 25Hz 正弦波のパターン電流で励磁される。これらを直接励磁した場合には膨大な無効電力が発生してしまうため，共振ネットワークを構築して励磁する。

電磁石は，12 のファミリーに分けられ，それぞれ独立に励磁される。このファミリー数は，これまでの加速器での実績である 3 ファミリーを遥かに超えている。このため，B/Q (BM, QM)間の磁場トラッキングをとることに困難が予想される。磁場トラッキングは，電磁石電源の通電パターン設定用の信号源に大きく依存するため，ダイナミックかつフレキシブルな信号発生器の開発が必要である。

このレポートでは，VXIbus を用いた信号発生器を提案する。VXIbus (VME eXtensions for Instrument) は，VMEbus の拡張であり，プロセス・バスおよびタイミングを共有するオープン・アーキテクチャを提供する。VXIbus を用いた信号発生器は，信号同期および多チャンネルを実現するために有利である。このため，信号発生器の所要性能を検討し，VXIbus を用いて信号発生器を構築した。さらに，実験を行い，基本オペレーションなどに関して所期の性能を確認した。

東海研究所：〒319-1195 茨城県那珂郡東海村白方白根 2-4
※ 外来研究員：(株)日立製作所
* 高エネルギー加速器研究機構

Contents

目次

1. Introduction

The 3 GeV proton synchrotron (3 GeV RCS) of the JAERI-KEK Joint Project (JKJ Project) for High-intensity Proton Accelerators [1] is a 25 Hz separate function rapid cycling synchrotron (RCS) that will be constructed at the JAERI Tokai site on schedule (Fig.1-1).

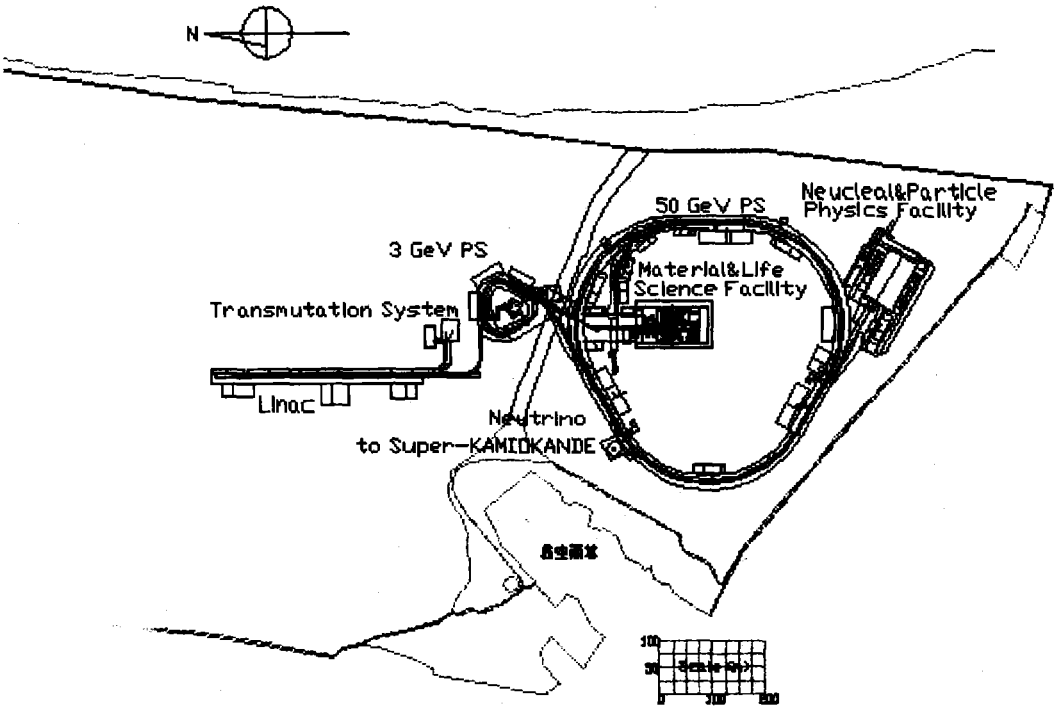

Fig. 1-1 Facility complex of the JAERI-KEK Joint Project for High-intensity Proton Accelerators

In a separate function RCS, magnetic excitation is carried out with bending magnets (BM) and quadrupole magnets (QM: QF or QD) in separate families. The three magnet families, BM, QF and QD, are excited either in one magnet string (e.g. ISIS 500 MeV Proton Synchrotron [2]) or in independent magnet strings (e.g. BESSY-II Electron Booster [3]). But for the 3 GeV RCS of the JKJ Project, above 10 magnet families are requested to excite independently [4], far beyond 3 families in practical RCS's constructed in the world. Difficulty of B/Q field tracking between BM and QM is significantly increased. B/Q tracking is an essential requirement for stabilizing the betatron tunes in a synchrotron by tracking the focusing (defocusing) magnetic field closely to the bending magnetic field. Since each magnet string is grouped into a resonant network and excited resonantly by a power supply typically with a DC-biased sinusoidal pattern as shown in Fig.1-2. Signal generator for the driving pattern of the power supply plays a crucial role in performing the field tracking between many magnet families.

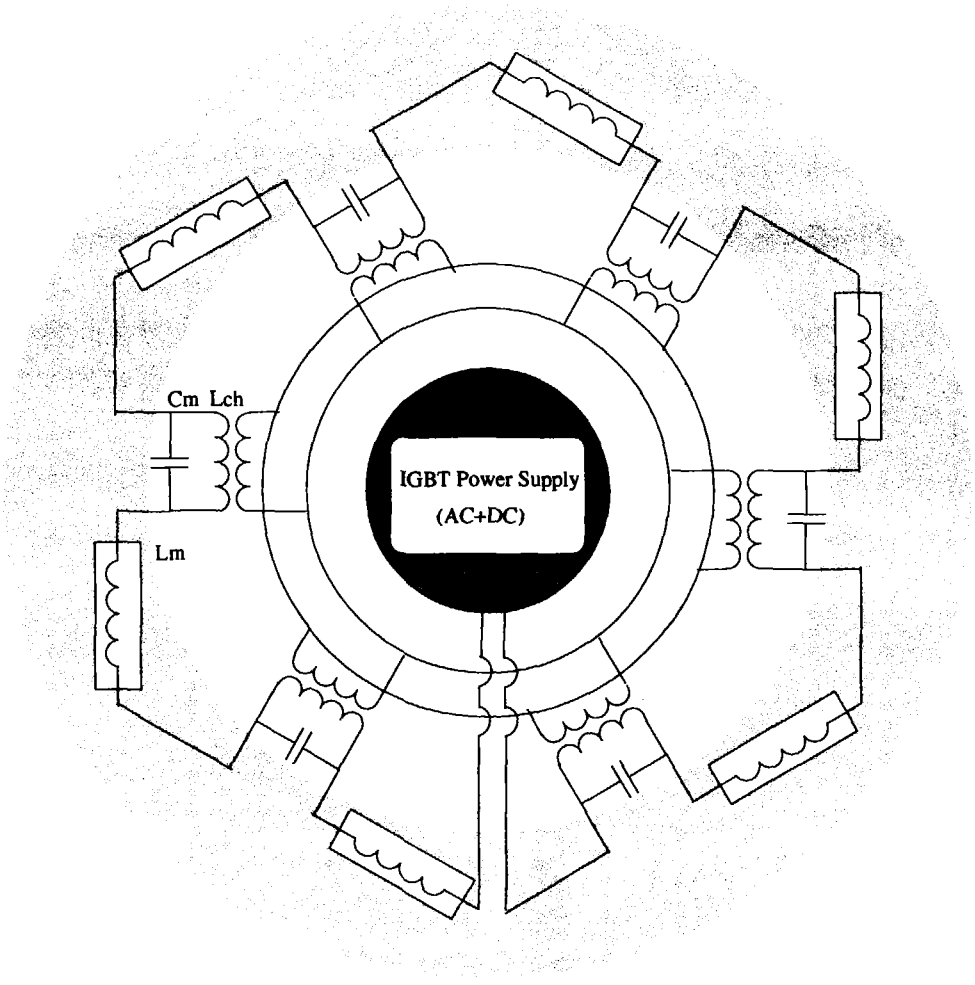

Fig. 1-2(a) One family of magnet string in resonant network and its power supply

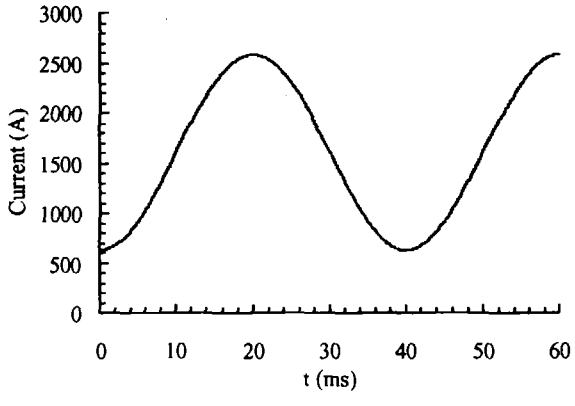

Fig. 1-2(b) Pattern of the power supply for bending magnets

To achieve close tracking, the driving signal of each power supply should be adjusted flexibly and dynamically in phase and amplitude. Waveform distortion, resulted from magnetic saturation, also contributes to the tracking errors, but the subject is not covered in this report. According to the proposed timing control of the 3 GeV RCS, the magnetic excitation is synchronized and triggered by a master trigger generated from the master clock of the accelerator complex [5]. Therefore the signal generator is obliged to have the following features.

- External trigger
- Dynamic phase adjustment (phase advance or lag)
- Dynamic amplitude adjustment
- Waveform adjustment without discontinuity
- Many channels
- etc.

This report introduces a VXIbus-based control system as illustrated in Fig. 1-3, and a signal generator is proposed for the resonant power supplies of the 3 GeV RCS.

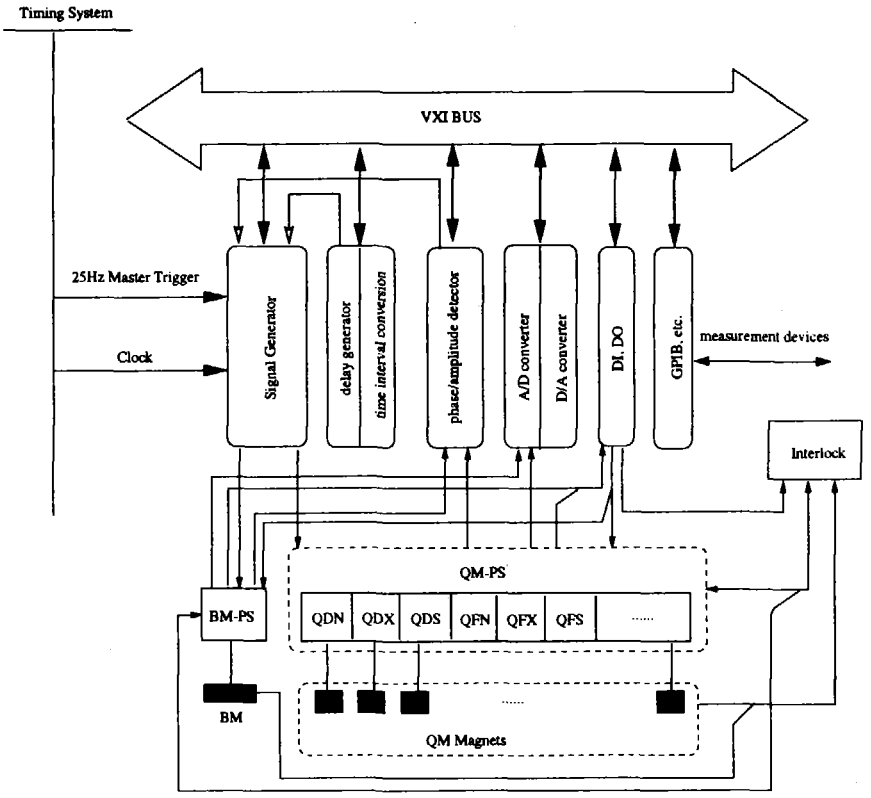

Fig. 1-3 Conceptual VXIbus-based control system proposed for resonant power supplies of the 3 GeV RCS

2. 3 GeV RCS Power Supply System for Lattice Magnets

The 3 GeV RCS accelerates a high-intensity proton beam from 400 MeV to 3 GeV at a repetition rate of 25 Hz. With designed beam power of 1 MW it will be used to produce pulsed spallation neutrons and muons and works as an injector as well for a 50 GeV synchrotron.

The magnetic field cycle repeats in the form of DC-biased sinusoidal pattern at 25 Hz as shown in Fig.1-2(b). To achieve a high intensity with low beam losses, betatron tunes, beam collimation, physical aperture and injection schemes are carefully designed and the present lattice version has a variety of features such as high transition gamma, long dispersion-free straight sections, etc. [4].

Bending magnet string and about 10 families of quadrupole magnets (QM's) are excited separately at a repetition rate of 25 Hz. The magnet string of each family is grouped into meshes and excited resonantly to avoid large amount of reactive power. Power supplies for above 10 families of main lattice magnets should be designed and be available on schedule for the construction of the accelerator complex. Based on the past R&D's [6,7], we are carrying on the design of the power supply system [8,9,10,11].

2.1 Tracking of Magnetic Field of Bending and Quadrupole Magnets

The magnetic field of each family of the QM's should closely track the BM field. The essential tracking requirement for synchrotron is described as follows [12].

$$\Delta\nu = \frac{1}{4\pi}\oint \Delta k\beta(s)ds = \frac{1}{4\pi}\oint \frac{\Delta k}{k}\cdot k\beta(s)ds \approx \frac{\Delta k}{k}\cdot\xi_{nature} \tag{2-1}$$

but

$$k = \frac{g}{B\rho} \tag{2-2}$$

where,

$\Delta\nu$: betatron tune shift,

k: quadrupole strength,

$\beta(s)$: betatron amplitude function,

ξ_{nature}: natural chromaticity,

g: field gradient of a quadrupole magnet,

B: magnetic field density of a bending magnet, and

ρ : bending radius of a bending magnet.

From above expressions, quadrupole strength k is required to keep constant during the operation cycle for injection, acceleration and extraction. The tune shift $\Delta\nu$, resulted from the quadrupole strength deviation is inevitable in practice due to deviation in phase and amplitude or due to waveform distortion.

We estimate the deviation resulted from phase and amplitude in field gradient of quadrupoles as described below.

BM field density (B) and QM field gradient (g) are given by:

$$g = g_{dc} - g_{ac} \cdot \cos(\omega_0 t) = g_{dc} \cdot (1 - \alpha \cdot \cos(\omega_0 t)) \tag{2-3a}$$

$$B = B_{dc} - B_{ac} \cdot \cos(\omega_0 t) = B_{dc} \cdot (1 - \alpha \cdot \cos(\omega_0 t)) \tag{2-3b}$$

We define

$$k_0 = \frac{g_{dc}}{B_{dc}\rho} = \frac{g_{ac}}{B_{ac}\rho}, \alpha = \frac{B_{ac}}{B_{dc}} = \frac{g_{ac}}{g_{dc}}$$

Assuming that QM field gradient (g) has phase error $\Delta\theta$ with respect to BM and amplitude error of Δg, we can derive the quadrupole strength deviation as follows.

$$(\frac{\Delta k}{k_0})_{\Delta\theta} \cong \frac{\alpha \cdot \sin(\omega_0 t)}{1 - \alpha \cdot \cos(\omega_0 t)} \cdot \Delta\theta \leq \frac{\alpha}{\sqrt{1-\alpha^2}} \cdot \Delta\theta \tag{2-4a}$$

$$(\frac{\Delta k}{k_0})_{\Delta g} = \frac{1}{1 - \alpha \cdot \cos(\omega_0 t)} \cdot \frac{\Delta g_{dc}}{g_{dc}} - \frac{\alpha \cdot \cos(\omega_0 t)}{1 - \alpha \cdot \cos(\omega_0 t)} \cdot \frac{\Delta g_{ac}}{g_{ac}}$$

$$(\frac{\Delta k}{k_0})_{\Delta g_{dc}} \leq \frac{1}{1-\alpha} \cdot \frac{\Delta g_{dc}}{g_{dc}}, (\frac{\Delta k}{k_0})_{\Delta g_{ac}} \leq \frac{\alpha}{1-\alpha} \cdot \frac{\Delta g_{ac}}{g_{ac}} \tag{2-4b}$$

Statistically, the deviation tolerance can be expressed as:

$$(\frac{\Delta k}{k_0})_{rms} = \sqrt{\frac{\alpha^2}{1-\alpha^2}\Delta\theta^2 + \frac{1}{(1-\alpha)^2} \cdot (\frac{\Delta g_{dc}}{g_{dc}})^2 + \frac{\alpha^2}{(1-\alpha)^2} \cdot (\frac{\Delta g_{ac}}{g_{ac}})^2} \tag{2-5}$$

Given ξ_{nature}=8.9 and α=0.61 in present design, the error tolerance can be estimated as shown in Fig. 2-1.

Supposing $(\frac{\Delta g_{dc}}{g_{dc}})_{rms} = (\frac{\Delta g_{ac}}{g_{ac}})_{rms} = 10^{-4}$, $\Delta\theta_{rms} \leqq 1.37$ mrad is required for $\Delta\nu \leqq 0.01$.

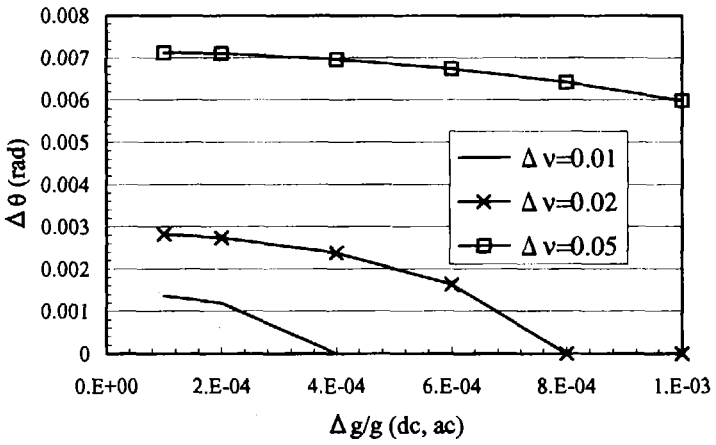

Fig. 2-1 Estimation of error tolerance for tune shift $\Delta\nu$=0.01, 0.02 and 0.05

2.2 Resonant Network Analyses

In an RCS, magnets are commonly configured as a resonant circuit named "White circuit", and powered by an AC power source [13]. The resonant current is generally DC-biased to achieve a full use of the sinusoidal waveform for beam injection and acceleration in one magnetic cycle. This general configuration of RCS avoids the generation of large amount of reactive power in magnet strings. Magnets are usually grouped into meshes to work at moderate resonant voltage. Each mesh is connected in series so that a uniform waveform in each magnet is achieved.

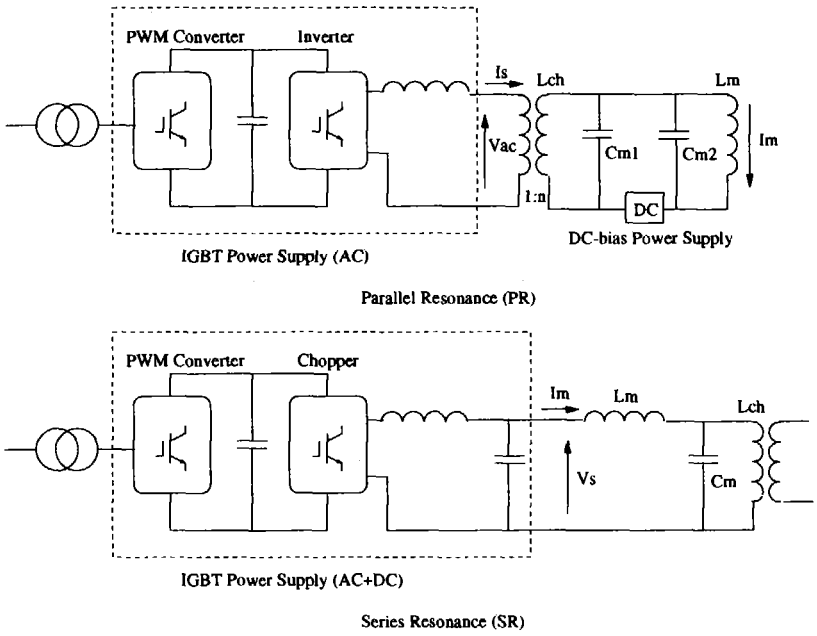

Fig. 2-2 Configuration of power supply system in parallel resonance (PR) or in series resonance (SR)

Figure 2-2 shows a one-mesh magnet/power supply configuration in RCS. An AC power source and a resonant circuit can be configured in parallel resonance (PR), or in a configuration variation with the power supply inserted in the resonant circuit in series (SR).

Fundamentally, the resonant network is driven by a current source (*I*s) in PR configuration or by a voltage source (*V*s) in SR configuration. With a simple AC model of the resonant circuit, circuit response is analyzed as follows.

The transfer function of the resonant circuit is

$$\frac{I_m}{I_s} = \frac{1}{n} \cdot \frac{{\omega_1}^2}{s^2 + (\frac{\omega_0}{Q})s + {\omega_0}^2} \qquad \text{for PR, (2-6a)}$$

or

$$\frac{I_m}{V_s} = \frac{1}{L_m s} \cdot \frac{s^2 + (\frac{\omega_0}{Q})s + {\omega_2}^2}{s^2 + (\frac{\omega_0}{Q})s + {\omega_0}^2} \qquad \text{for SR, (2-6b)}$$

where, ${\omega_0}^2 = \frac{L_m + L_{ch}}{L_m L_{ch} C_m}$ is the resonant frequency, $Q = \omega_0 C_m R_e = \frac{R_e \cdot (L_{ch} + L_m)}{\omega_0 L_{ch} L_m}$ is the quality factor of the resonant circuit, ${\omega_1}^2 = \frac{1}{L_m C_m}$, ${\omega_2}^2 = \frac{1}{L_{ch} C_m}$, R_e is the equivalent resistance for AC losses and 1:n =turns ratio (primary/secondary) of the choke transformer in PR.

Phase of the transfer function is derived in eqs. (2-7) for PR and SR respectively:

$$\phi(\frac{I_m}{I_s}) = -\arctan[\frac{\omega_0 \omega}{Q({\omega_0}^2 - \omega^2)}] \qquad \text{for PR (2-7a)}$$

or

$$\phi(\frac{I_m}{V_s}) = \arctan[\frac{\omega_0 \omega}{Q({\omega_2}^2 - \omega^2)}] - \arctan[\frac{\omega_0 \omega}{Q({\omega_0}^2 - \omega^2)}] - \frac{\pi}{2} \qquad \text{for SR (2-7b)}$$

Therefore,

$$\Delta\phi = \frac{\partial\phi}{\partial\omega_0}\Delta\omega_0 + \frac{\partial\phi}{\partial Q}\Delta Q = -\frac{Q\omega\cdot((\omega_0{}^2-\omega^2)-2\omega_0{}^2)\cdot\Delta\omega_0 - \omega_0\omega(\omega_0{}^2-\omega^2)\cdot\Delta Q}{Q^2(\omega_0{}^2-\omega^2)^2+(\omega\omega_0)^2}$$

$$\Delta\phi(\omega_0) = \frac{2Q}{\omega_0}\cdot\Delta\omega_0 \qquad \text{at } \omega=\omega_0 \text{ for PR,} \quad (2\text{-}8a)$$

or, for SR, we have

$$\Delta\phi = \frac{\partial\phi}{\partial\omega_0}\Delta\omega_0 + \frac{\partial\phi}{\partial Q}\Delta Q$$

$$= \frac{Q\omega\cdot(\omega_2{}^2-\omega^2)\cdot\Delta\omega_0 - \omega_0\omega(\omega_2{}^2-\omega^2)\cdot\Delta Q}{Q^2(\omega_2{}^2-\omega^2)^2+(\omega\omega_0)^2}$$
$$- \frac{Q\omega\cdot((\omega_0{}^2-\omega^2)-2\omega_0{}^2)\cdot\Delta\omega_0 - \omega_0\omega(\omega_0{}^2-\omega^2)\cdot\Delta Q}{Q^2(\omega_0{}^2-\omega^2)^2+(\omega\omega_0)^2}$$

At $\omega=\omega_0$, we get

$$\Delta\phi(\omega_0) = \frac{Q\omega_0\cdot(\omega_2{}^2-\omega_0{}^2)\cdot\Delta\omega_0 - \omega_0{}^2(\omega_2{}^2-\omega_0{}^2)\cdot\Delta Q}{Q^2(\omega_2{}^2-\omega_0{}^2)^2+\omega_0{}^4} + \frac{2Q}{\omega_0}\cdot\Delta\omega_0$$

Supposing $L_{ch}=k*L_m$, we get $\omega_0{}^2=(1+k)\cdot\omega_2{}^2$, and therefore

$$\Delta\phi(\omega_0) = (-\frac{k(1+k)}{(kQ)^2+(1+k)^2}+2)\cdot\frac{Q}{\omega_0}\cdot\Delta\omega_0 - \frac{k(1+k)}{(kQ)^2+(1+k)^2}\cdot\Delta Q \cong 2Q\cdot(\frac{\Delta\omega}{\omega_0}) \qquad (2\text{-}8b)$$

Response to a step signal helps us to understand the performances in real time.

In PR, we get

$$I_m(s) = \frac{1}{n}\cdot\frac{\omega_1{}^2}{s^2+(\frac{\omega_0}{Q})s+\omega_0{}^2}\cdot\frac{1}{s} = \frac{1}{n}\cdot(\frac{-\frac{\omega_1{}^2}{\omega_0}(\frac{1}{\omega_0}\cdot s+\frac{1}{Q})}{s^2+(\frac{\omega_0}{Q})s+\omega_0{}^2}+\frac{\frac{\omega_1^2}{\omega_0^2}}{s})$$

and

$$I_m(t) = \frac{1}{n} \cdot (\frac{\omega_1}{\omega_0})^2 \cdot (1 - e^{-\frac{\omega_0}{2Q}t} \frac{2Q}{\sqrt{4Q^2 - 1}} \cdot \cos(\sqrt{1 - \frac{1}{4Q^2}} \cdot \omega_0 t - \varphi)) \qquad (2\text{-}9a)$$

but $\varphi = \arctan(\frac{1}{\sqrt{4Q^2 - 1}})$.

Similarly, in SR we obtain

$$I_m(s) = \frac{1}{L_m s} \cdot \frac{s^2 + (\frac{\omega_0}{Q})s + {\omega_2}^2}{s^2 + (\frac{\omega_0}{Q})s + {\omega_0}^2} \cdot \frac{1}{s} = \frac{1}{L_m} \cdot (\frac{(1 - \frac{\omega_2^2}{\omega_0^2}) \cdot (-\frac{s}{\omega_0 Q} + (1 - \frac{1}{Q^2}))}{s^2 + (\frac{\omega_0}{Q})s + {\omega_0}^2} + \frac{(1 - \frac{\omega_2^2}{\omega_0^2}) \cdot \frac{s}{\omega_0 Q} + \frac{\omega_2^2}{\omega_0^2}}{s^2})$$

and

$$I_m(t) = \frac{1}{L_m} \cdot (\frac{(1 - \frac{\omega_2^2}{\omega_0^2})}{\omega_0 Q}(1 - e^{-\frac{\omega_0}{2Q}t} \cdot \sqrt{1 + \frac{(2Q^2 - 1)^2}{4Q^2 - 1}} \cdot \cos(\omega_0 \sqrt{1 - \frac{1}{4Q^2}} t + \varphi)) + \frac{\omega_2^2}{\omega_0^2} \cdot t) \qquad (2\text{-}9a)$$

but, $\varphi = \arctan(\frac{2Q^2 - 1}{\sqrt{4Q^2 - 1}})$.

(Notice: the terms of the equations related to the response to DC component is not in correct form due to the transfer function is based on AC equivalent circuit.).

From the expressions derived above, we can describe the circuit responses with network parameters, i.e. quality factor Q and resonant frequency ω_0. The analyses help us to understand the performances of the resonant circuits, some of which can be concluded as below.

- Phase shift due to resonant frequency variation: $\Delta\phi(\omega_0) = 2Q \cdot (\frac{\Delta\omega_0}{\omega_0})$
- Time constant of amplitude variation for resonant current $\tau = \frac{2Q}{\omega_0}$
- $\omega_0 = \sqrt{\frac{L_m + L_{ch}}{L_m L_{cm} C_m}}, Q = \omega_0 C_m R_e = \frac{R_e \cdot (L_{ch} + L_m)}{\omega_0 L_{ch} L_m}$

3. VXIbus-based Control System

3.1 Introduction to VXIbus

VXIbus (VME extensions for Instrument) is a fast-growing platform for instrument systems [14]. Because of many limitations in VME specifications-particularly for analog conversion, the major instrument manufactures developed the specifications for VXIbus, and VXIbus was adopted as IEEE Standard 1155 in March 1993. VXI is now used in many applications ranging from test and measurement and ATE (Automatic Test Equipment), to data acquisition and analysis in both research and industrial automation.

VXI-an open architecture with shared process bus and timing (Fig.3-1) offers the numerous benefits below.

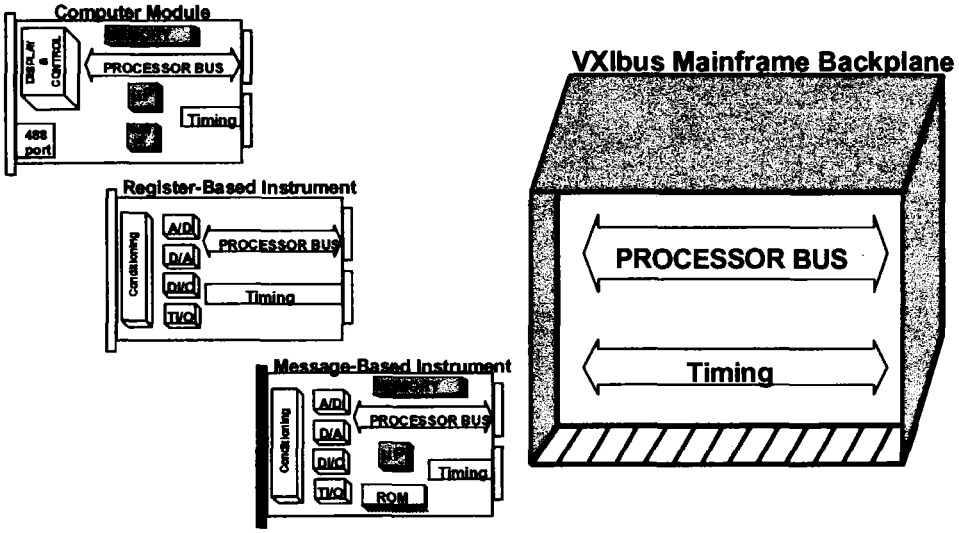

Fig.3-1 VXI: an open architecture with shared process bus and timing

- Open standard with extensive multivendor support from many of largest instrument suppliers, including National Instruments, Hewlett-Packard and Tektronix, etc.
- Modular approach for system configuration with off-the-shelf building blocks that meet specific application needs.
- Easy programming and integration with standardized VXIplug&play software because of standards for both hardware and software combined by the VXI Consortium and VXIplug&play System Alliance.
- A precision clock for timing and trigger lines for event handling-to facilitate high-performance systems.
- Increased system throughput reduces test time and increases capabilities.

- Mechanical configuration with smaller size and higher density facilitates mobility or portability and access to the test and control devices.

To support the open multivendor architecture, members of VXIplug&play Systems Alliance [15] have implemented common standards in both hardware and software. All hardware that is compatible with the VXIbus Specifications is applicable to VXIplug&play frameworks. The alliance also achieves interoperability for system software including operating system, programming language, I/O drivers, instrument drivers and higher-level application software tools.

3.2 Access to VXIbus Device

VXIbus devices are configured and accessed by the following ways.

1). Hardware Registers

VXI modules have a specific set of registers for hardware configuration. The following is the description of VXI configuration registers.

- Upper 16kB of A16 space reserved for VXI configuration space
- 64B per device
- 8-bit logical address specifies base address for each device
- 256 devices per VXI system

Each VXI device has an 8-bit logical address, which is analogous to GPIB address of a GPIB device and can be manually set or automatically configured by the system at startup.

2). Register-based Devices

With VXI configuration registers-the common register set for all VXI devices, the system can identify each VXI device (its type, model/manufacturer, address space, and memory requirements). System and memory configuration can be performed automatically with the Resource Manager (RM), a centralized soft module for system initialization.

3). Message-based Communication and Word Serial Protocol

VXIbus specification defines message-based devices in addition to register-based devices. All message-based VXIbus devices have communication register and configuration registers and can communicate at a minimum level in a standard way using VXI-specific Word Serial Protocol, which is very similar to IEEE-488 protocol.

4) Commander/Servant Hierarchies

VXI Commander/Servant Hierarchies is a communication protocol using conceptual layers of VXI devices to construct hierarchical system. The structure is like an inverted tree in which a Commander device has one or more associated lower-level Servant devices. Commanders communicate with Servants through communication registers of Message-based servants using the Word Serial Protocol or by device-specific register manipulation for Register-based servants. Servants communicate with their Commander by responding to the Word Serial commands and queries, or by device-specific register status.

5). Interrupts and Asynchronous Events

Servants can communicate asynchronous status and events to their Commander through hardware interrupts or by writing specific messages (signals) directly to their Commander's hardware Signal Register.

3.3 Ways to Control a VXI System

Slot 0 controllers provide the communication path between other modules in the mainframe and its host computer. Slot 0 controllers can be divided into three categories:

1). GPIB-VXI interface module: The GPIB-VXI interface transparently translates the GPIB protocol to and from the VXI Word Serial protocol.

2). Embedded Controller: this is an embedded computer module offering direct connection to VXI backplane.

3). MXIbus (Multisystem eXtensions for Instrumentation bus): MXIbus links an external computer to control the VXI backplane. The external computer operates as though it is embedded directly inside the VXI mainframe.

3.4 VXIbus Interface Software

1). VISA: Virtual Instrument System Architecture

As a standard I/O Application Programming Interface (API) for instrumentation programmings defined by the VXIplug&play Systems Alliance, VISA can control VXI, GPIB, PXI or serial instruments for either message-based communication or register-based communication.

2). IVI: Interchangeable Virtual Instruments

Interchangeable Virtual Instruments defined more standardization to instrument drivers and can do instrument simulation [16]. Interchangeability is achieved through generic class drivers such as oscilloscope, DMM, arbitrary waveform/function generator, switch and power supply, in which an instrument is controlled by using a set of function and attributions.

4. Signal Generator Scheme and Experiment

Signal generators to drive RCS magnet power supplies differ in accelerator facilities since requested tracking tolerance is not the same and each facility has different development story. We introduce the schemes of two existing RCS's in BESSY II (Berlin, Germany) and SRRC (Hsinchu, Taiwan) before going into the details of the scheme proposed for the 3 GeV RCS.

4.1 Signal Generator Scheme for BESSY II and SRRC

BESSY II and SRRC are both 3rd generation synchrotron radiation light sources in which RCS boosters are used to shorten beam filling time. Both are excited at 10 Hz from injection energy of 50 MeV to extraction energy of 1.5 GeV (BESSY II) and 1.9 GeV (SRRC) respectively and either drives three independent 10 Hz White circuits for dipoles and two quadrupole families. Since the absolute tracking tolerance may differ each other, BESSY II booster synchrotron adopted Dual Arbitrary Waveform Generator ADS, a commercial signal generator by Rohde&Schwarz and a circuitry unit is implemented for magnetic field regulation and phase synchronization. On the other hand, in recent upgrade SRRC developed a VME module for 10 Hz signal generator with control interface for phase and amplitude control. Table 1 is a brief comparison of the signal generators of BESSY II Booster, SRRC booster and the proposed 3 GeV RCS [3,4,17,18].

Table 1 A comparison of the signal generator schemes for BESSY-II, SRRC and 3GeV RCS

	BESSY II Booster	SRRC Booster	3 GeV RCS (proposal)
Frequency (Hz)	10	10	25
Family number	3	3	11
Timing reference	B field	B field	Master trigger (ext.)
Signal generator	Rohde&Schwarz ADS	VMEbus-based	VXIbus-based
Interface function	Phase/amplitude control	Phase/amplitude control	Phase/amplitude control
Tune shift	<0.05	Unknown	<0.01

4.2. Signal Generator Scheme Proposed for the 3 GeV RCS

In the proposed control system shown in Fig.1-3, a VXI module (Wavetek Model 1375) is used as the signal generator. It is triggered and synchronized by a 25 Hz master trigger signal obtained from a tentative timing system. The other blocks are functioned with VXI modules or with software implementation as follows.

1). Signal generator: Wavetek Model 1375 20 MS/s Arbitrary Waveform Generator, triggered and synchronized (externally) by master trigger signal.

2). Phase delay (or advance) block: the phase delay (or advance) is carried out by memory shift of the sinusoidal pattern instead of using converter circuit.

3). Time interval converter: time interval is measured and obtained directly using Hp E1333A (counter).

4). Software environment: LabVIEW [19].

Figure 4-1 illustrates the programming flow diagram and the control scheme of the system. Omitting the DC-bias, we create the sinusoidal pattern with the following memory data:

$$(2^{12}-1)\cdot[1+\sin(2\pi\cdot\frac{n-\frac{N-M}{2}}{M})]/2, n=0,1,2,...,N-1$$

where, N is the memory length, M ($<N$) is the length for one repetition period, and the 12-bit vertical data ranges from minimum through maximum with the midpoint corresponding the zero of the sinusoidal pattern. The signal generator outputs one period of data with memory shift index p as the start point, namely:

$$(2^{12}-1)\cdot[1+\sin(2\pi\cdot\frac{n-\frac{N-M}{2}}{M})]/2, n=p,p+1,p+2,...,p+M-1$$

where p=[0, N-M].

The signal phase can be shifted by $\pm\frac{N-M}{2}\cdot\frac{2\pi}{M}$ with step of $\frac{2\pi}{M}$ as shown in Fig.4-1(a). Signal patterns M_0, M_1 and M_2 illustrates typically the cases for in phase, phase advance and phase lag respectively.

Occurring upon the request from the external trigger, the VXI Events process the adjustments of the phase and amplitude of the waveform so that the adjustments can be carried out with correct timing in defined time interval. As shown in Fig.4-1(b), the scheme enables the events to be counted to KE and phase and amplitude adjustments are applied at Event No.KA and KB respectively.

4.3 Experiment

An experimental set of the VXI-based signal generator is built to confirm the scheme and performances. Figure 4-2 shows the external trigger, external clock and the output signal.

Limited by the memory size of 32 kB of the module, pattern memory is set to 25000 data points among which 20000 points are outputted for one repetition period and 5000 points left for memory shift. Accordingly, the external clock is set to 500 kHz synchronized by the external clock of 25 Hz. The phase of the output signal can be shifted for 1.26 radian (10 ms) with minimum step of 0.314 mrad (2 μs).

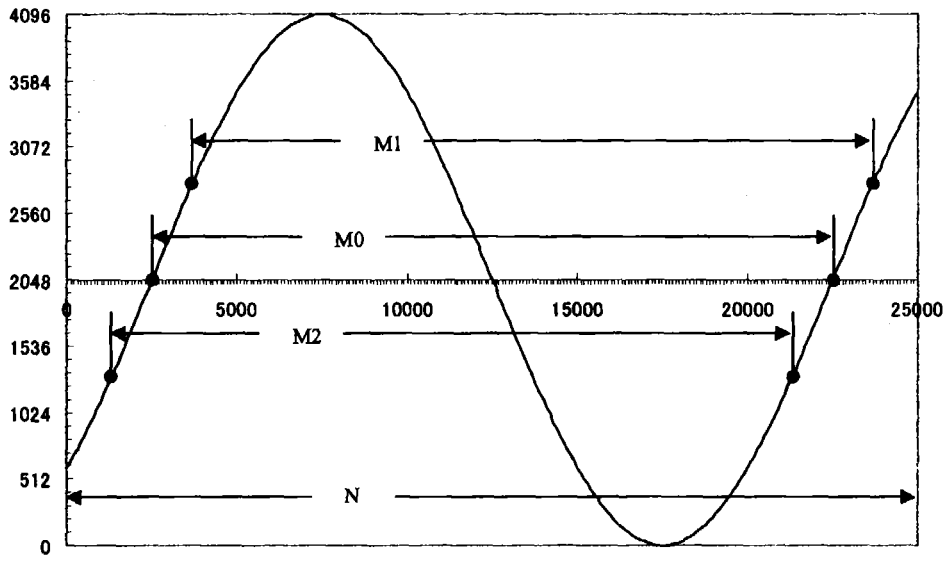

Fig.4-1 (a) Memory data of sinusoidal pattern

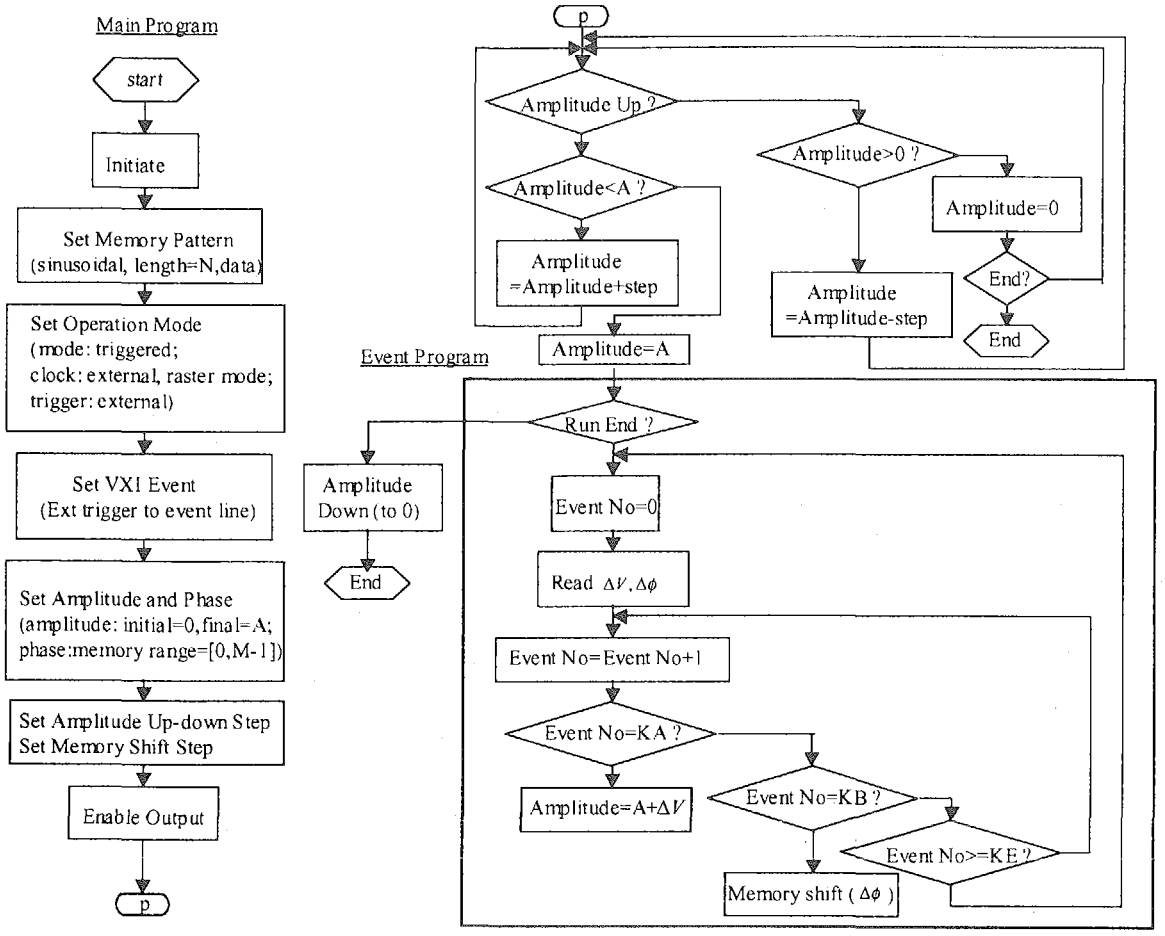

Fig.4-1 (b) Flow diagram

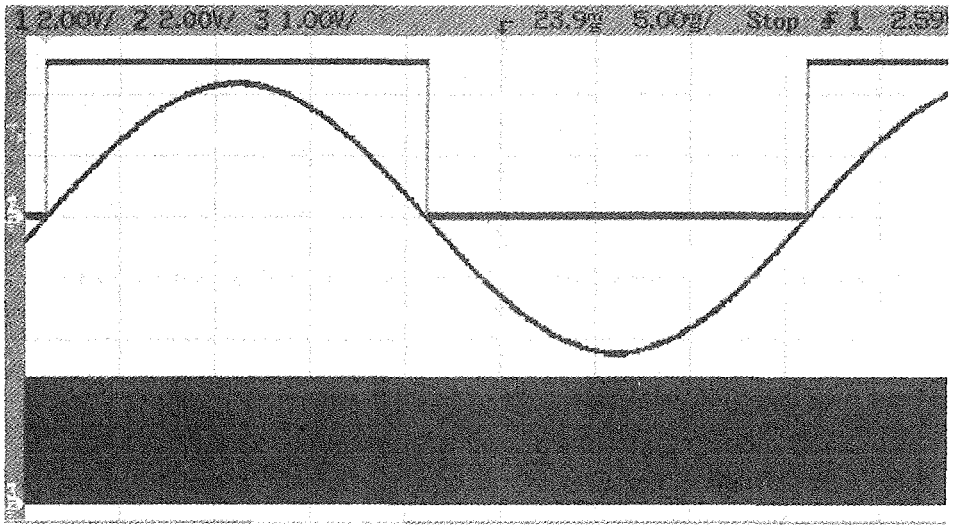

Fig.4-2 External trigger (top), output signal (middle) and external clock (bottom), horizontal: 5 ms/div

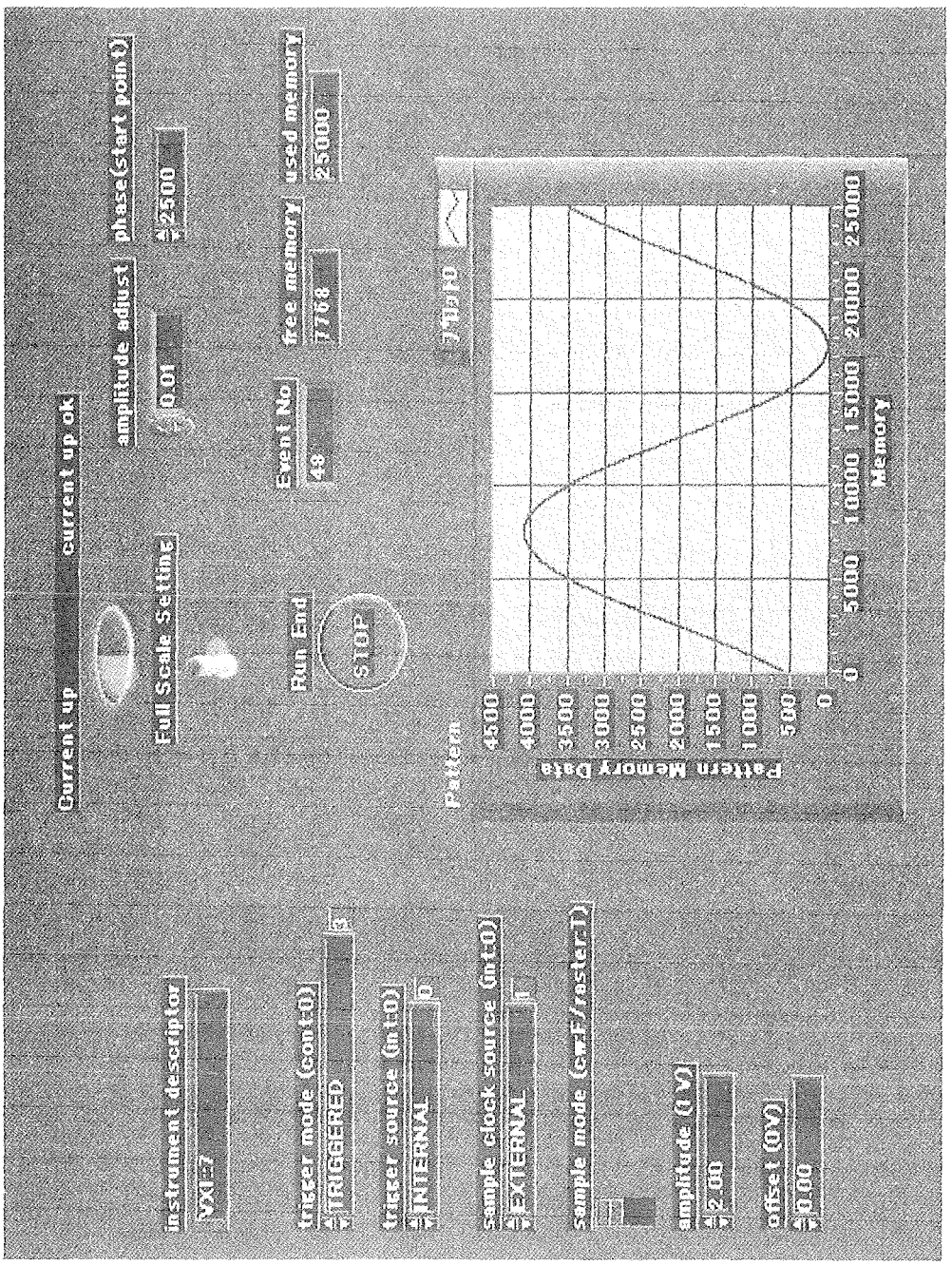

Fig. 4-3 Front panel of the signal generator

Figure 4-3 is the LabVIEW front panel of the signal generator. Wavetek Model 1375 is indicated by instrument descriptor VXI::7. And this instrument can be extended to many channels. After trigger mode/source and sample clock source/sample mode are set, the signal generator is started up in sequence defined as in the figure.

Startup and shutdown of the signal generator are shown in Fig. 4-4. The rise and fall time can be set according to practical use. After the output reaches the set value, amplitude regulation and phase shift are functioned.

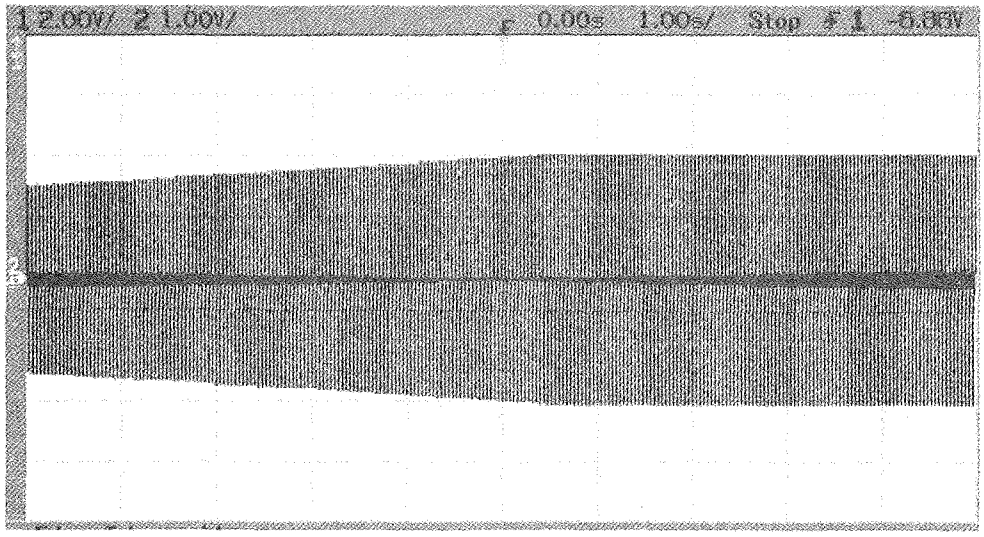

Fig.4-4 (a) Signal output at start-up (horizontal: 1s/div)

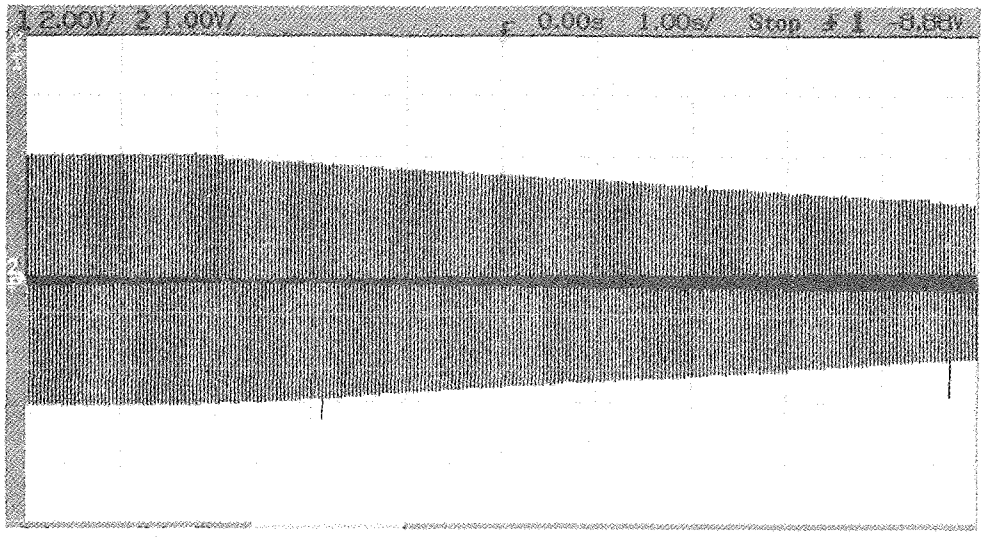

Fig. 4-4(b) Signal output at shutdown (horizontal: 1 s/div)

Figure 4-5 demonstrates three cases of the phase shift, i.e. phase lag, in phase and phase advance, with respect to the external trigger signal. Since the phase shift is controlled by memory shift, the phase shift is operated precisely.

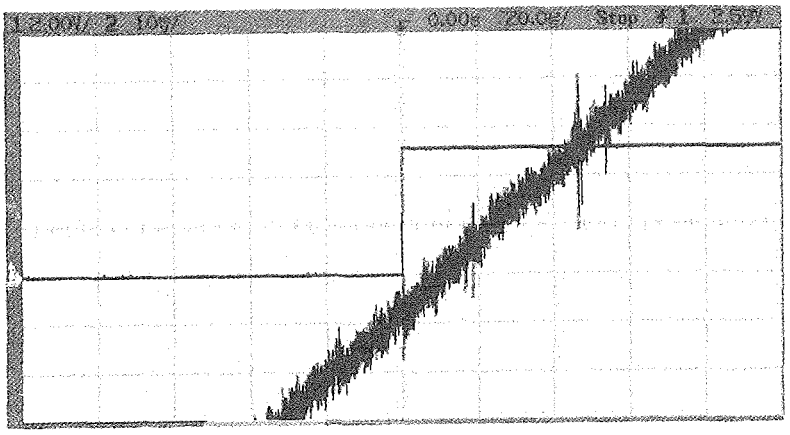

(a) phase lag of 10 μs

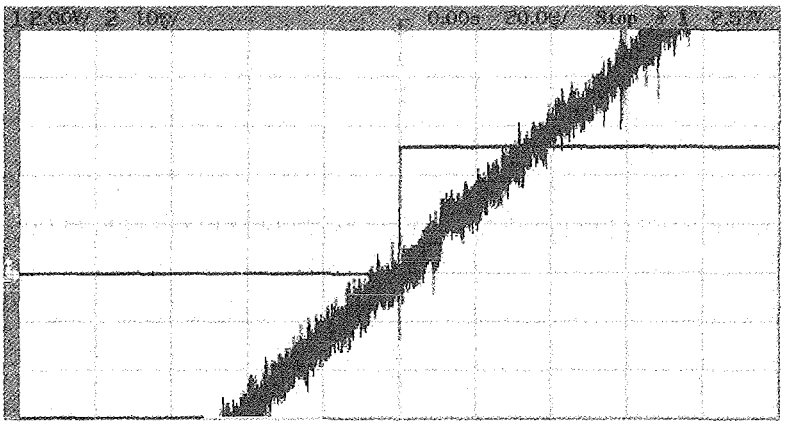

(b) in phase

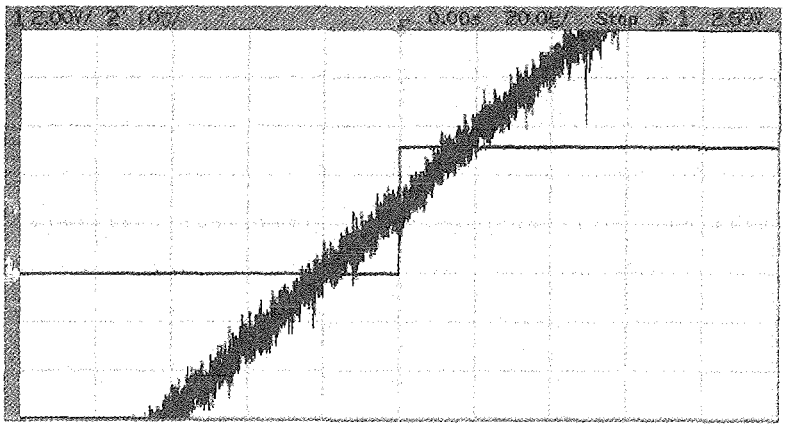

(c) phase advance of 20 μs

Fig.4-5 Signal output phase with respect to external trigger signal (horizontal: 20 μs/div)

A model power supply [6] was used to test the performance of the signal generator and the functions have been well demonstrated.

5. Conclusions

The VXIbus-based signal generator provides a way to drive the resonant power supplies for the main magnets of the 3 GeV RCS. Experiments have confirmed the operation. Flexible adjustments in both phase and amplitude of waveform facilitate the close B/Q tracking between many magnet families. For better adjustment accuracy, it is preferred to upgrade the DAC of the VXI module to16-bit and extend the memory points to over 1M. Further experiments are planed to fulfill the feedback control in amplitude regulation and phase synchronization.

Acknowledgements

We are grateful to Hideaki YOKOMIZO, director of Center for Neutron Science, Hiromitsu SUZUKI, subgroup leader of Accelerator Group and Prof. Yoshiro IRIE from KEK for supporting this research work.

References

[1] The Joint Project Team of JAERI and KEK, "The Joint Project for High-Intensity Proton Accelerators", JAERI-TECH 99-056, or KEK Report 99-04, JHF-99-3 (1999).

[2] B. Boardman, "Spallation Neutron Source: Description of Accelerator and Target", RL-82-006 (1982).

[3] M. Abo-Bakr, et al., "The BESSY II Booster Synchrotron", EPAC 96, Barcelona, (1996).

[4] http://jkj.tokai.jaeri.go.jp/

[5] C. Ohmori, Y. Mori, et al., "JKJ Accelerator Timing System", 15th Meeting of the International Collaboration on Advanced Neutron Sources (ICANS-XV), Tsukuba, Japan (2000).

[6] F.Q. Zhang, T. Adachi, H. Someya, "Recent Development of a Magnet Power Supply for a Rapid-Cycling Synchrotron at KEK", KEK Report 2000-5, May 2000.

[7] M. Muto, et al., "A Magnet Power Supply in Series Resonance", KEK Proc. 99-20 (in Japanese), Jan. 2000.

[8] F.Q. Zhang, et al., "Resonant magnet power supply system for the 3 GeV synchrotron of the JAERI-KEK Joint Project", Proc.of 6th Symp. on Power Supply Tech. for Accelerators, also JAERI-J 17994, (2000).

[9] F.Q. Zhang, et al., "Resonant and Pulsed Magnet Power Supplies for the 3 GeV Synchrotron of the JAERI-KEK Joint Project", 18th International Conference On High Energy Accelerators (2001).

[10] S. Koseki, et al., "Study of Resonant Magnet Exciting System for the 3 GeV Proton Synchrotron ", in Japanese, Denki Gakkai (2001).

[11] Y. Watanabe, et al., "Magnet Power Supply of a 3 GeV Proton Synchrotron", in Japanese, Denki Gakkai (2001).

[12] S.Y. Lee, Accelerator Physics, World Scientific (1999).

[13] M.G. White, et al., "A 3-BeV High Intensity Proton Synchrotron", The Princeton-Pennsylvania Accelerator, CERN Symp. 1956 Proc., p525.

[14] http://www.vxi.org/

[15] http://www.vxipnp.org/

[16] http://www.ivifoundation.org/

[17] K. Bürkmann, et al., "Performance of the White Circuits of the BESSY II Booster Synchrotron", EPAC 98, Stockholm, (1998).

[18] R.C. Sah, J.R. Chen, et al., "Operations and Upgrades at SRRC", Proc. of EPAC 2000, Vienna, (2000).

[19] LabVIEW Measurements Manual, National Instruments.

This is a blank page.

国際単位系 (SI) と換算表

表 1　SI 基本単位および補助単位

量	名称	記号
長さ	メートル	m
質量	キログラム	kg
時間	秒	s
電流	アンペア	A
熱力学温度	ケルビン	K
物質量	モル	mol
光度	カンデラ	cd
平面角	ラジアン	rad
立体角	ステラジアン	sr

表 2　SI と併用される単位

名称	記号
分，時，日	min, h, d
度，分，秒	°, ′, ″
リットル	l, L
トン	t
電子ボルト	eV
原子質量単位	u

1 eV = 1.60218 × 10^{-19} J

1 u = 1.66054 × 10^{-27} kg

表 5　SI 接頭語

倍数	接頭語	記号
10^{18}	エクサ	E
10^{15}	ペタ	P
10^{12}	テラ	T
10^{9}	ギガ	G
10^{6}	メガ	M
10^{3}	キロ	k
10^{2}	ヘクト	h
10^{1}	デカ	da
10^{-1}	デシ	d
10^{-2}	センチ	c
10^{-3}	ミリ	m
10^{-6}	マイクロ	μ
10^{-9}	ナノ	n
10^{-12}	ピコ	p
10^{-15}	フェムト	f
10^{-18}	アト	a

表 3　固有の名称をもつ SI 組立単位

量	名称	記号	他の SI 単位による表現
周波数	ヘルツ	Hz	s^{-1}
力	ニュートン	N	m·kg/s^2
圧力，応力	パスカル	Pa	N/m^2
エネルギー，仕事，熱量	ジュール	J	N·m
工率，放射束	ワット	W	J/s
電気量，電荷	クーロン	C	A·s
電位，電圧，起電力	ボルト	V	W/A
静電容量	ファラド	F	C/V
電気抵抗	オーム	Ω	V/A
コンダクタンス	ジーメンス	S	A/V
磁束	ウェーバ	Wb	V·s
磁束密度	テスラ	T	Wb/m^2
インダクタンス	ヘンリー	H	Wb/A
セルシウス温度	セルシウス度	℃	
光束	ルーメン	lm	cd·sr
照度	ルクス	lx	lm/m^2
放射能	ベクレル	Bq	s^{-1}
吸収線量	グレイ	Gy	J/kg
線量当量	シーベルト	Sv	J/kg

表 4　SI と共に暫定的に維持される単位

名称	記号
オングストローム	Å
バーン	b
バール	bar
ガル	Gal
キュリー	Ci
レントゲン	R
ラド	rad
レム	rem

1 Å = 0.1 nm = 10^{-10} m

1 b = 100 fm^2 = 10^{-28} m^2

1 bar = 0.1 MPa = 10^5 Pa

1 Gal = 1 cm/s^2 = 10^{-2} m/s^2

1 Ci = 3.7 × 10^{10} Bq

1 R = 2.58 × 10^{-4} C/kg

1 rad = 1 cGy = 10^{-2} Gy

1 rem = 1 cSv = 10^{-2} Sv

（注）

1. 表 1 — 5 は「国際単位系」第 5 版，国際度量衡局 1985 年刊行による。ただし，1 eV および 1 u の値は CODATA の 1986 年推奨値によった。
2. 表 4 には海里，ノット，アール，ヘクタールも含まれているが日常の単位なのでここでは省略した。
3. bar は，JIS では流体の圧力を表わす場合に限り表 2 のカテゴリーに分類されている。
4. EC 閣僚理事会指令では bar，barn および「血圧の単位」mmHg を表 2 のカテゴリーに入れている。

換算表

力

N(=10^5 dyn)	kgf	lbf
1	0.101972	0.224809
9.80665	1	2.20462
4.44822	0.453592	1

粘度　1 Pa·s(N·s/m^2) = 10 P(ポアズ)(g/(cm·s))

動粘度　1 m^2/s = 10^4 St(ストークス)(cm^2/s)

圧力

MPa(=10 bar)	kgf/cm^2	atm	mmHg(Torr)	lbf/in^2(psi)
1	10.1972	9.86923	7.50062 × 10^3	145.038
0.0980665	1	0.967841	735.559	14.2233
0.101325	1.03323	1	760	14.6959
1.33322 × 10^{-4}	1.35951 × 10^{-3}	1.31579 × 10^{-3}	1	1.93368 × 10^{-2}
6.89476 × 10^{-3}	7.03070 × 10^{-2}	6.80460 × 10^{-2}	51.7149	1

エネルギー・仕事・熱量

J(=10^7 erg)	kgf·m	kW·h	cal(計量法)	Btu	ft·lbf	eV
1	0.101972	2.77778 × 10^{-7}	0.238889	9.47813 × 10^{-4}	0.737562	6.24150 × 10^{18}
9.80665	1	2.72407 × 10^{-6}	2.34270	9.29487 × 10^{-3}	7.23301	6.12082 × 10^{19}
3.6 × 10^6	3.67098 × 10^5	1	8.59999 × 10^5	3412.13	2.65522 × 10^6	2.24694 × 10^{25}
4.18605	0.426858	1.16279 × 10^{-6}	1	3.96759 × 10^{-3}	3.08747	2.61272 × 10^{19}
1055.06	107.586	2.93072 × 10^{-4}	252.042	1	778.172	6.58515 × 10^{21}
1.35582	0.138255	3.76616 × 10^{-7}	0.323890	1.28506 × 10^{-3}	1	8.46233 × 10^{18}
1.60218 × 10^{-19}	1.63377 × 10^{-20}	4.45050 × 10^{-26}	3.82743 × 10^{-20}	1.51857 × 10^{-22}	1.18171 × 10^{-19}	1

1 cal = 4.18605 J (計量法)
= 4.184 J (熱化学)
= 4.1855 J (15 °C)
= 4.1868 J (国際蒸気表)

仕事率　1 PS (仏馬力)
= 75 kgf·m/s
= 735.499 W

放射能

Bq	Ci
1	2.70270 × 10^{-11}
3.7 × 10^{10}	1

吸収線量

Gy	rad
1	100
0.01	1

照射線量

C/kg	R
1	3876
2.58 × 10^{-4}	1

線量当量

Sv	rem
1	100
0.01	1

(86 年 12 月 26 日現在)

VXIbus-based Signal Generator for Resonant Power Supply System of the 3 GeV RCS